

Conversion (OTEC) systems, crude oil transport, evaporators, chemical reactors, nuclear stations, food industry installations. They account for a basic case of open channel-flow studies. Film liquid is generally characterized by the presence of instabilities, adding more complexity to its thickness measurements.

The techniques devoted to falling film thickness measurements should have two essential qualities: precision and sensitivity to variations. The latter would increase the results accuracy since ripples may appear on the liquid free surface. Several experimental methods based on various physics phenomena were developed including electrical properties variations (resistivity and capacitance), light reflection and refraction, photography, acoustic waves reflection and absorption of rays (gamma and x-rays).

Pioneer work, reported by Kapitza and Kapitza [1], had used photography of shadows to avoid light reflection effects, caused by liquid interface on image acquisition, to study various wavy flow regimes on the surface of a liquid film falling over an inclined plane. Özgü et al. [2] developed a method based on electrical capacitor variations to measure the liquid thickness in presence of a bubble in a vertical tube with 2.94 cm of inner diameter. The authors didn't take into account the temperature impact, on the liquid electrical conductivity and the metallic probe, as well as the bubble effect which could affect the measured thickness. Fukano [3] pointed out that the technique based on electrical properties variations presents another flaw with the existence of signal saturation during acquisition causing then a loss of information. For that purpose, Selegim and Hervieu [4] proposed to use a high frequency signal at the entrance to minimize the impedance of the liquid around the probes. Therefore, in order to solve the above cited problems, Klausner et al. [5] developed a liquid deepness measurement method, deduced from electrical capacitor. The authors proposed a correlation including temperature effect on measured thickness within a range of 20 °C to 200 °C. In addition, they used their technique to study evaporation of a liquid film of R113 in rectangular cavity.

The intrusive techniques may create local perturbation that will affect the measurements especially in case of a study on the apparition of natural instability. Hurlburt and Newell [6] created an optical technique using total light reflection by liquid interface. They used a monochromatic laser beam split, by a special coating layer, into two beams giving then two measuring positions leading to a mean value of wave celerity along the channel. The film thickness was deduced by measuring the radius variations between the reflected laser beams (after photographing them with a video camera). However, the obtained light points were not totally circular. Thus, by using the mean radius values, the authors increased the error on the liquid depth and wave's velocity. The idea of the reflected laser beams was interesting though limited to transparent liquids, because the laser was sent from the bottom of the

channel. Furthermore, by taking a mean value of the wave celerity the variations of the latter were hidden. Another inaccuracy was noted on the radius measurement on the recorded images. Shedd and Newell [7] improved the method developed by Hurlburt and Newell [6] using a specific signal processing on the recorded images obtaining a better precision on the measured liquid film thickness. The same authors [8] used this method to study two-phase flow in three channels of different shapes (circular, triangular and rectangular). The liquid deepness results compared well to those obtained by Hurlburt and Newell [6].

Zhang et al. [9] proposed a method using light absorption by a liquid film flow in laminar and turbulent regimes. A laser sheet lighting a liquid layer was used and light intensity was measured using a photodiode. The liquid film thickness variations were deduced after processing the electrical signal. The results were in good agreement with those obtained using the correlation given by Chang et al. [10] for a thickness ranging from 0.4 mm to 0.9 mm.

Liu et al. [11] used fluorescence technique to measure film thickness variations and wave dynamics at the film surface. The authors confirmed the theory of Benjamin [12] defining a critical Reynolds number beyond which wavy instabilities appear on the film surface. De Olivera et al. [13] used an optical technique based on light attenuation to measure the liquid film thickness in an open channel flow. This non-intrusive technique, available for translucent fluid, allowed recordings with approximately an error of 7%. Wegener and Drallmeier [14], reported film thickness measurements accomplished with a method called "Laser Focus Displacement". This technique allowed these authors to follow the time dependent interface oscillations with a good precision as long as the wavy regime is not too strong.

Tibiriçà et al. [15] gathered, in his article, the most important experimental methods in measuring liquid film thickness variations. The authors classified all these techniques according to the physics involved including ultrasonic, laser absorbance, x-rays as well as intrusive methods (electrical conduction, capacitance variations).

According to the literature survey, all the reported measurements were conducted locally at one point with a fairly appreciable precision. In order to record the film thickness distribution, as well as some dynamical properties of the fluid, it would be appropriate to make measurements at several positions instantaneously which constitute the main contribution of the present work. The method, developed and reported hereafter, aims to bring some improvements to the drawbacks pointed out previously. Furthermore, the technique is independent of the properties of the fluid with no need to inject particle or tracing powders. It gives access to thickness variations and to the most important parameters dealing with wave's dynamics traveling on liquid interface. The technique is validated, in case of liquid film with flat interface, by two methods,

experimental and theoretical as it will be discussed in this paper. In case of a wavy liquid film, the method is assessed using an experimental setup developed and devoted to such test.

The capabilities of this experimental technique are enlightened through the investigation of a liquid film flowing over an inclined plane.

Material and Methods

Experimental Loop and Measurement Technique

The experimental method is a non-intrusive technique based on the reflection of laser beams due to the difference of refractive index between the studied liquid film and the ambient medium (air in our case). The experimental loop used is shown in Fig. 1(a). The liquid film flows over an inclined plane at a constant mass flow rate. The liquid is introduced by 8 injectors (Fig. 1(d)) distributed uniformly along the width of the channel. A gate is put at the inlet (Fig. 1(d)) unifying the flow level, eliminating the injection effect, inducing then a gravity driven flow. The channel was sufficiently wide to neglect all the side boundaries effects on the film flow, as it will be shown at a later stage, and can be considered as a two-dimensional flow. The liquid is stored in a tank and injected again in the channel by a pump. A scheme and a picture of the experimental set-up are shown in Fig. 1(a) and (e) respectively.

A 1 mW laser source, of 632.8 nm wave-length, was used. Semi-reflective mirrors split the laser beam into six rays. The measurement technique was based on the reflection of a laser beam by the liquid surface. Each beam crossed a diaphragm, eliminating residual rays, and a converging lens to impinge the top of a very thin Plexiglas plate as shown in Fig. 1(c). The ray was reflected, partly by the plate (first light spot), and by the liquid interface giving second bright spot on the screen. The second light spot will follow the liquid interface displacements (Fig. 1(b)). The size of the laser spots recovered by image processing was found to have a maximum value of 0.1 mm. The liquid film thickness was deduced from the distance separating both spots. The motion of the six laser spots was recorded with a camera controlled by a computer. The acquisition frequency, according to the work of Shkadov [16] obeys the Nyquist–Shannon [17] sampling theorem (i.e: $f_c > 2 f_{max}$). The processed videos lead to the film thickness evolution at six positions. A raw image sample for an instable flow case is provided in Fig. 1(b).

The oscillations of a light spot were caused by the presence of waves in case of unstable flow regime. It should be mentioned that natural waves, on liquid film surface, have very small amplitude compared to the wave length (according to the results of Kapitza and Kapitza [1], Shkadov [16] and Liu

et al. [11]). For that purpose, the surface was taken flat neglecting the local curvature. The liquid film thickness was deduced from the distance between the two laser spots for both stable and instable flow regimes (flat and wavy interface). The incidence angle (i) was fixed before starting measurements. Noting in Fig. 1(c) that the two points E and F , on the screen, are recorded and shown in Fig. 1(b) and the distance EF is then measured and related to the thickness of the film as follows:

$$h(x, t) = L - BC \quad (1)$$

L is the distance (in “mm”) separating both plates (that is between the lower surface of the upper plate and the upper face of the lower plate). Taking into account that the measured distance EF is given by:

$$EF = E_1C = E_1E_2 + E_2B + BC = E_1E_2 + \tau + BC \quad (2)$$

where τ is the thickness of the upper plate. Noting that $\tan(i) = \frac{AE_2}{E_1E_2}$ and AE_2 can be expressed as:

$$AE_2 = AA' + A'E_2 = \tau \times \tan(r) + BC \times \tan(i) \quad (3)$$

We deduce E_1E_2 as:

$$E_1E_2 = \frac{AE_2}{\tan(i)} = \left\{ \tau \times \frac{\tan(r)}{\tan(i)} + BC \right\} \quad (4)$$

Substituting equation (4) into equation (2) yields:

$$EF = \tau \left(1 + \frac{\tan(r)}{\tan(i)} \right) + 2 \times BC \quad (5)$$

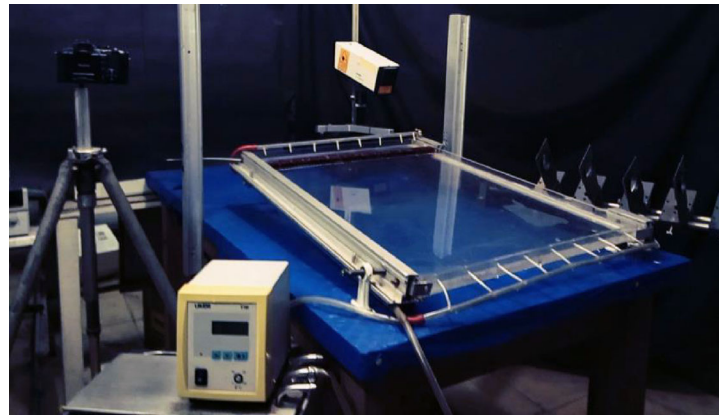
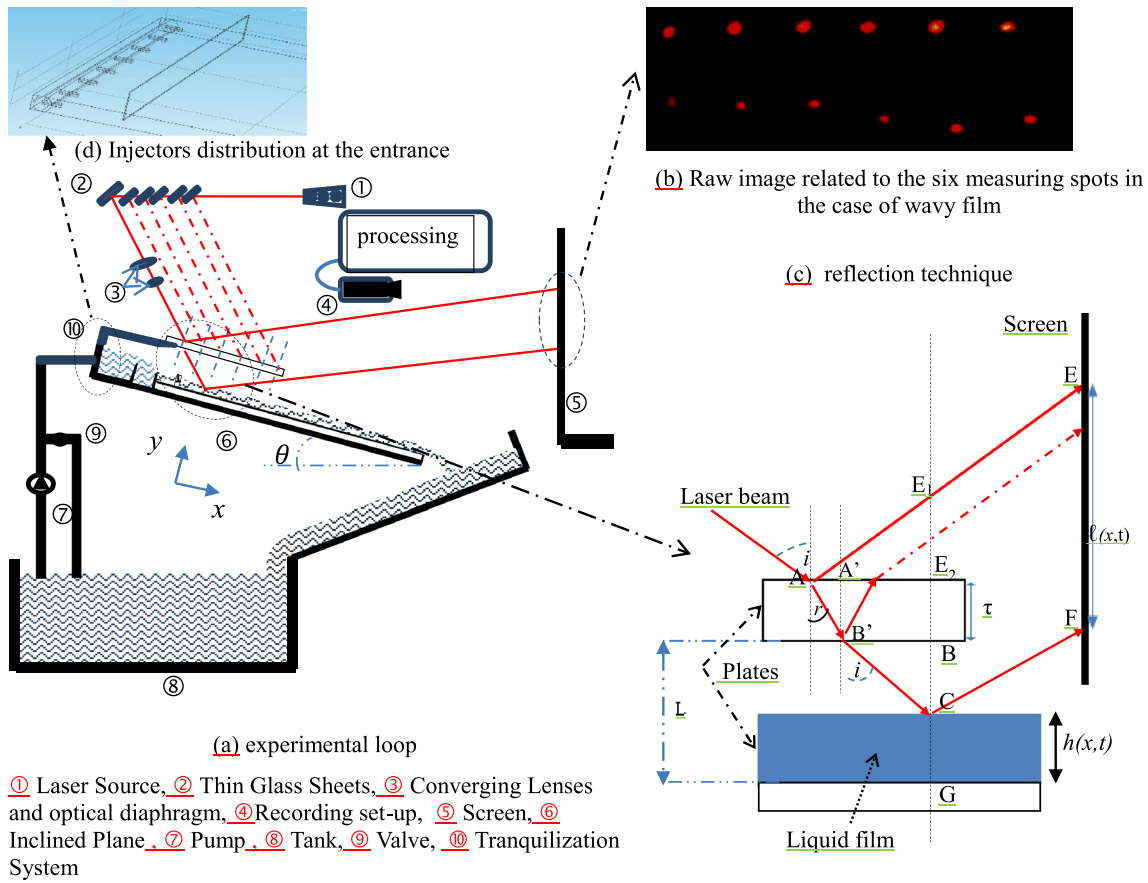
Recall:

$$n_1 \times \sin(i) = n_2 \times \sin(r) \quad (6)$$

i is the incident angle while r is the refracted angle, n_1 and n_2 are the reflective indices of the air and the plate respectively.

From equation (6) we get:

$$\begin{aligned} \tan(r) &= \frac{\frac{n_1}{n_2} \times \sin(i)}{\sqrt{1 - \left(\frac{n_1}{n_2} \times \sin(i)\right)^2}} \rightarrow \frac{\tan(r)}{\tan(i)} \\ &= \frac{\frac{n_1}{n_2} \times \cos(i)}{\sqrt{1 - \left(\frac{n_1}{n_2} \times \sin(i)\right)^2}} \end{aligned} \quad (7)$$



(e) experimental stand

Fig. 1 Experimental set-up

Substituting equation (7) into equation (5) and setting $EF = \ell$ we can obtain an expression for BC the distance between the surface of the liquid and the lower surface of the upper plate as:

$$BC = \frac{1}{2} \left\{ \ell(x, t) - \tau \left(1 + \frac{\frac{n_1}{n_2} \times \cos(i)}{\sqrt{1 - \left(\frac{n_1}{n_2} \times \sin(i)\right)^2}} \right) \right\} \quad (8)$$

ℓ expresses the recorded distance between E and F on the screen given in millimeters; in fact ℓ is a function of space

and time: $\ell = f(x, t)$. The thickness of the upper plate τ is also measured in “mm”. Finally, the film thickness (equation (1)) is computed as follows:

$$h(x, t) = L - \frac{1}{2} \left\{ \ell(x, t) - e \left(1 + \frac{\frac{n_1}{n_2} \times \cos(i)}{\sqrt{1 - \left(\frac{n_1}{n_2} \times \sin(i)\right)^2}} \right) \right\} \quad (9)$$

The incidence angle (i) was fixed at 13 degrees with an accuracy of 0.1° and readjusted at each new value of the inclination angle θ . The reflective index of the plate was measured and found to be equals to $n_2 = 1.493$ while the reflective index of air is taken as $n_1 = 1$. The upper plate thickness was also measured and yields to $\tau = 0.406 \pm 0.006$ mm. Thus equation (9) was then expressed in “mm” as:

$$h(x, t) = L - \frac{1}{2} \{ \ell(x, t) - 0.674 \} \quad (10)$$

‘The recorded videos are treated using a series of software, they are transformed to series of images using “XnConvert” software as a first step (a sample image is given on Fig. 1(b)), where The grey level is plotted on each single image of the obtained series using “imageJ” software which allows to detect laser spots position very precisely. This processing presents two sources of errors: e_{spot} and e_{scale} . The image processing generates an error on spot position related to video-camera resolution. The error on the film thickness measurements could be affected by the scaling (e_{scale}), the sensor (e_{sensor}) and the image resolution (e_{spot}) that is:

$$e_{\text{tot}} = e_{\text{sensor}} + e_{\text{spot}} + e_{\text{scale}} \quad (11)$$

The scaling required was achieved by a micrometric system measurement leading to an error of $e_{\text{scale}} = 2$ μm . The number of pixels on the camera’s CCD sensor led to an error of 4 μm evaluated as follows:

$$e_{\text{sensor}} = \frac{\text{Pixels number on y axes of sensor}}{\text{sensor's real size along "y axes"}} \quad (12)$$

Additionally, the images processing induced, by the camera resolution, an error on a spot position $e_{\text{spot}} = P_{\text{SZ}} = 32$ μm equals to a pixel’s size, computed as:

$$P_{\text{sz}} = \frac{\text{Pixels number on "y axes"}}{\text{Image real length along "y axes"}} \quad (13)$$

Where P_{sz} represents the real size (length) of one pixel on the treated images, this size depends on the camera resolution (pixels number on ‘yy’ axis’) and the total real length of the image on the “y” axis.

Finally, taking into account the uncertainty on the plate thickness an absolute error of 44 μm accuracy is obtained which, in fact, appears to be fairly acceptable for a one millimeter liquid film thickness. Based on several pioneer works [1, 10–12, 14] and other applications including plane photo-bioreactors, food industry, oil transport and some chemical reactors this accuracy is judged to be

acceptable. It should be mentioned this accuracy is related to pixels number calculated for a standard video camera (1280×720 pixels). This can be minimized using a camera with a higher number of pixels.

Alternative Methods and Assessment

The measurements, obtained with the laser reflection technique, were assessed with the Spectroscopic Ellipsometry (S.E.) Woollam et al. [18], in case of stable film (flat interface) and by an additional optical setup called here after expansion method in case of unstable film.

The stable liquid film flow, characterized by a flat interface with a constant local thickness “h”, can be assimilated to a solid sheet with a uniform thickness. For that purpose, the Spectroscopic Ellipsometry (S.E.) technique was used to check the accuracy of the experimental data. Furthermore, the S.E. technique presents a Nano-scale error.

The Spectroscopic Ellipsometry (S.E.) is an optical measurement technique that characterizes light reflection (or transmission) from samples. The key feature is the measure of changes on polarized light upon light reflection or transmission by a sample. Ellipsometry measures the amplitude ratio ψ and phase difference Δ between light waves known as -p and -s- polarized light waves (Fig. 2). In S.E. spectra (ψ and Δ) are measured by changing the wavelength of light. In general, the spectroscopic ellipsometry measurement is carried out in the ultraviolet visible region, but measurements in the infrared region have also been performed widely [18].

The steps required to make S.E. measurements can be summarized as follows: a glass plate is deposited on a silicon wafer; the analyzer and the detector are positioned at an angle of 75° ; then the sample position is adjusted to collect the maximum reflected light intensity, whose polarization is elliptical. The data giving the variations of $\tan(\psi)$, $\cos(\theta)$ and other parameters, depending on the wavelength, are recorded and analyzed with the SEA 1.2.44 software.

When the interface is slightly wavy the expansion method is used to assess the data. This technique is based on the extension of an object by a set of lenses while keeping the resolution of the acquired image or video by a camera presenting a frequency of 30 fps (CFM = 30 Hz) as shown in Fig. 3. The lenses were first tested on the image sharpness to avoid any chromatic aberrations. A zoom effect was first used, to minimize the size of one pixel which will reduce the error on the film’s interface position giving a higher accuracy on the thickness measurement, then a second lens, based on microscope principle, giving an extended image with a good contrast. The Laser Multi-Reflection approach is used at the same time and same position with expansion method in order to measure the thickness variation in case of wavy liquid film as shown in Fig. 3(a). A Sample raw image obtained by this method is provided in Fig. 3(b). Similarly the error associated

Fig. 2 Spectroscopic Ellipsometry Measurement System SEMILAB GES-5E



on the thickness (e_{tot}) could be affected by the scaling ($e_{scale} = 2 \mu m$), the sensor (e_{sensor} given by equation (12)), that is $4 \mu m$, and the interface position related to image resolution ($e_{interface}$) = $P_{SZ} = 15 \mu m$ giving a final error of $e_{tot} = 21 \mu m$.

Results and Discussion

Data Validation

Experimental validation

Nine (9) solid samples were measured by the three above described techniques. The Spectroscopic Ellipsometry technique will be considered as reference scale hereafter. The control samples had thicknesses ranging from 0.14 mm to 3.17 mm measured by S.E. with a maximum average error of 0.05%. The accuracy for the reflection and expansion methods were quantified (see Fig. 4) by computing the relative errors “ e_{LMRM} ” as: $e_{LMRM} = 100 * \frac{E_{LMRM} - E_{S.E.}}{E_{S.E.}}$ with E_{LMRM} being the measured samples thickness by the Laser Multi-Reflection Method (LMRM). This relative error is also calculated for the Expansion Method as: $e_{EX} = 100 * \frac{E_{EX} - E_{S.E.}}{E_{S.E.}}$, where E_{EX} and $E_{S.E.}$ are respectively the samples thickness

measured by the Expansion Method and the Spectroscopic Ellipsometry. Both methods (Fig. 4) present a good accuracy with a relative error not exceeding 3.5%. This error becomes negligible as the thickness increases.

The expansion method remains a limited local technique and doesn't give access to all parameters dealing with the interface dynamics. But, as depicted in Fig. 4, its high accuracy, on liquid film thickness measurement, makes this technique an acceptable candidate in the assessment of the Laser Multi-Reflection approach in case of wavy liquid film. For that purpose a series of synchronized measurements of the liquid interface deformation induced by a wave, created artificially with a wave generator, were made using both experimental techniques at one point “M” in the channel (Fig. 3). The mean deviation resulting from measurements, made by both techniques as seen in Fig. 5, was less than 5% assessing then the multi-reflection technique accuracy.

Comparison with theoretical prediction

An assessment of the reflection technique was also made with the Nusselt [19] model giving, for a one-dimensional gravity driven liquid film flow on an inclined plan, a relation between the volume flow rate

Fig. 3 The expansion method

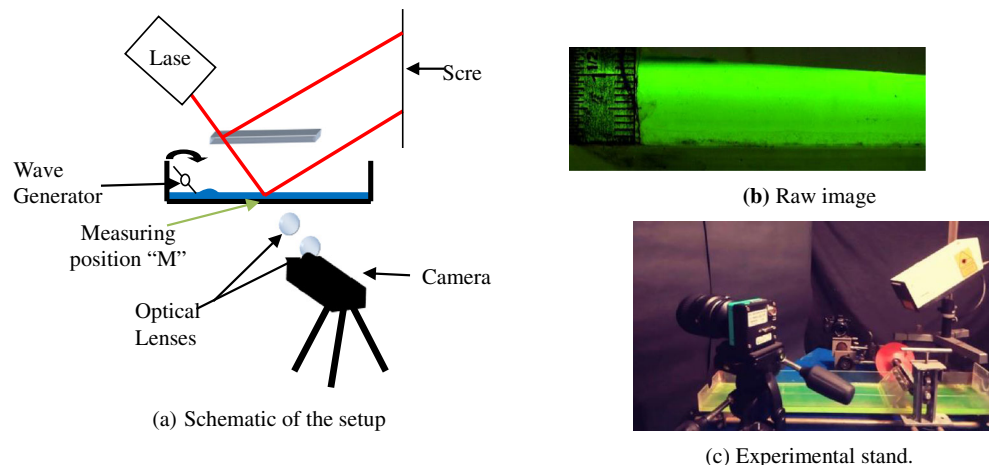
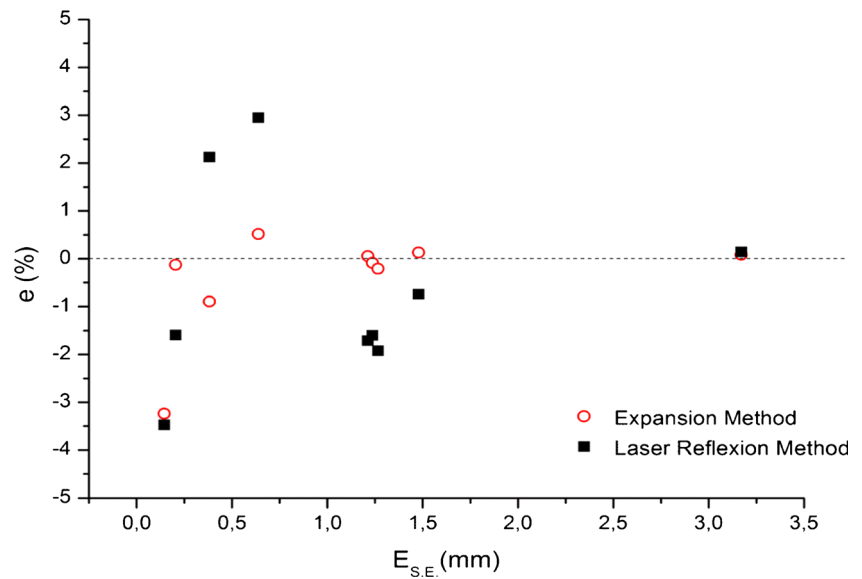


Fig. 4 Relative errors “ e_{Cam} and e_{Reflec} ” for the expansion and laser reflection techniques



Q_v , the inclination angle θ , the kinematic viscosity ν and the liquid thickness h_n as follows:

$$h_n = \left(\frac{3\nu}{g \sin \theta} Q_v \right)^{\frac{1}{3}} \quad (14)$$

Figure 6 shows a very good agreement, for a stable liquid film at various Reynolds number and inclinations, between theory and experiments. A maximum relative gap of 4% was recorded.

Highlights on the Multi-Reflection Technique

The laser beams were sent from the top to eliminate light absorption by the liquid layer. Thus, the present technique could be used for any liquid film independently of its density, whether it is homogeneous and isotropic or not, which is not the case of the light absorption methods. Moreover, the two reflected laser beams, leading to the thickness measurement (equations (9) or (10)), are clearly distant from each other. This technique, independent of light intensity variation, doesn't require any spot's mean radius measurement Hurlburt and Newell [6] that would introduce additional error. Furthermore, in case of particle laden liquid film the presence of particles (or surface scattering) may affect the light intensity of the laser Hanrahan [20]; without disturbing the position of the center of the spot.

Compared to the methods based on light intensity variations, this technique doesn't require any intensity measurement. Therefore, the error related to light attenuation, external noise on photodiodes or the output signal saturation is eliminated. Compared to LFD (Laser Focus Displacement) technique used by Lan et al.

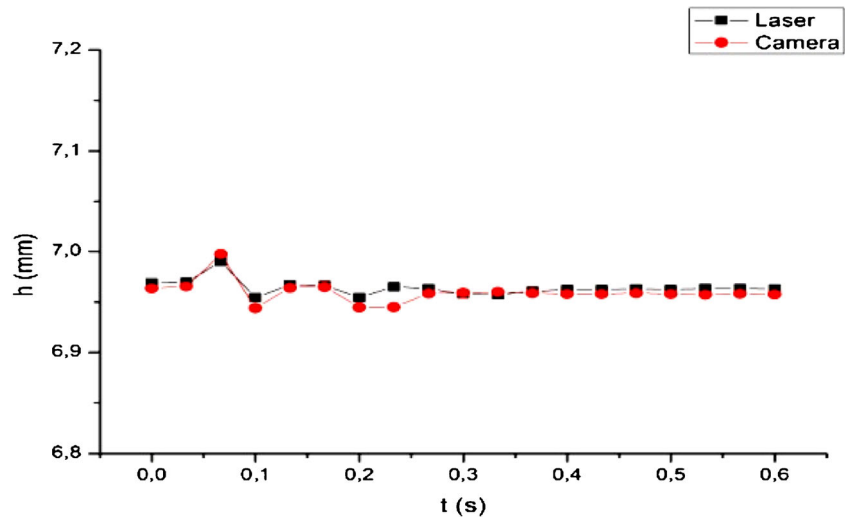
[21], the present method doesn't depend on any oscillation frequency. In addition, interferences are avoided since the laser beams doesn't cross each other (Fig. 1). The methods using PIV or Fluorescence are definitely very useful however, in case of thin liquid film, the injection of particles or fluorescent powder might affect the apparition of instability and transition between wavy regimes at the interface.

Finally splitting the laser source into several beams allows measuring the film thickness at several locations instantaneously in addition to other important parameters dealing with wave's dynamics (amplitude, celerity, wave length, form and class). Other techniques will give a punctual information. For stable liquid films, the flow mean velocity can be deduced from the values of thickness at the six measurement points using Nusselt expression, given then more details about gravity and surface tension effects on film flow.

The liquid thickness is measured with an error of 44 μm which is less than 5% in case of 1 mm film thickness. The accuracy depends on liquid layer thickness and can be better for thicker films. One of the most important advantages of the present technique is the sensitivity to the smallest interface deformations that may appear the independence on the film temperature. One should note the high accuracy, obtained after a specific image processing, on the recordings of the liquid thickness oscillations especially in instable regime.

The present technique can be very applied in various cases including film thickness distribution and temporal variation, for plane photo-bioreactors [22]: a critical data affecting the output of the bioreactor for mass production; as well as tracking (in some cases) the interface in solidification problems.

Fig. 5 Validation test for the film thickness measurements given by both techniques



Measurements on the Liquid Film Flow

Film thickness

The influence of the side boundaries was first checked by measuring the film thickness at four locations (Fig. 7). One should note that, for a given x -position, the film thickness remains roughly the same. Therefore, the channel can be considered wide enough to neglect the side boundaries effect. The film was then approximated as being a two-dimensional flow.

The film thickness measurements were then conducted at six locations for various Reynolds numbers and inclination angles. A sample of the liquid film evolution is shown in Fig. 8(a) for a Reynolds number of 25.7. The measured, mean value of the film thickness was then compared to the Nusselt's model (equation (9)) giving rise to a relative discrepancy, called E (equation (10)), as shown in Fig. 7(b).

$$E (\%) = 100 * \frac{h_{\text{measured}} - h_n}{h_n} \quad (15)$$

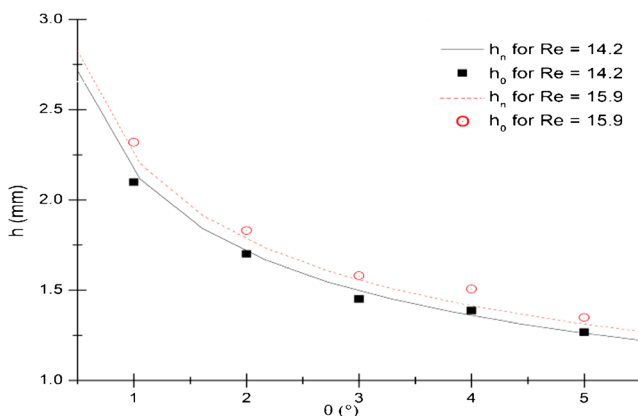


Fig. 6 Comparison between the Nusselt's model and experiments for stable liquid film flow

The discrepancy (gap) between theory and the experimental data (Fig. 8(b)) was evaluated for all Reynolds numbers and inclination angles used in this investigation. The values of E did not exceed 5% for $Re \leq 27$ and $\theta = 1^\circ$ and 2° as well as for $Re \leq 16$ and $\theta = 3^\circ$. Figure 8(b) can be used to deduce the domain of validity of equation (9) with suitable accuracy. This could be seen as an assessment of the Nusselt's expression for a flow with a primary instability. For instance, if a limit of 10% is selected the prediction would be still adequate as long as $Re \leq 16$ and $\theta \leq 10^\circ$. However, for $Re > 16$ the theoretical prediction would be acceptable for $\theta \leq 2^\circ$; higher inclinations would induce errors exceeding 10%. In fact, the instabilities become significant for $Re > 16$ and $\theta > 3^\circ$ affecting the mean value of the film height.

The average value of the film thickness was plotted for various Reynolds numbers and inclination angles. As expected the average liquid film thickness decreases with the inclination angle θ as depicted in Fig. 9.

Instability threshold

The instability threshold and the wave dynamics depends on the inclination angle and Reynolds number for a gravity driven liquid film. Measurements (Fig. 10) were conducted within the same range of inclination angles considered by Liu et al. [11]. The critical Reynolds number values, obtained were slightly higher than those measured by the latter and those predicted by Benjamin [12] and those measured by Liu et al. [11]. The theoretical analysis considered in the works of Benjamin [12], Gjevik [23] and other similar articles, used linear stability analysis. The latter introduced some approximations and the equations could be solved with linear analysis or weakly non-linear method. However, the results led to a similar formulation of Benjamin [12].

The experimental technique used in the present work has the advantage of being non-intrusive which means that there

Fig. 7 Boundary effect on the film thickness distribution. (a) measuring locations; (b) film thickness

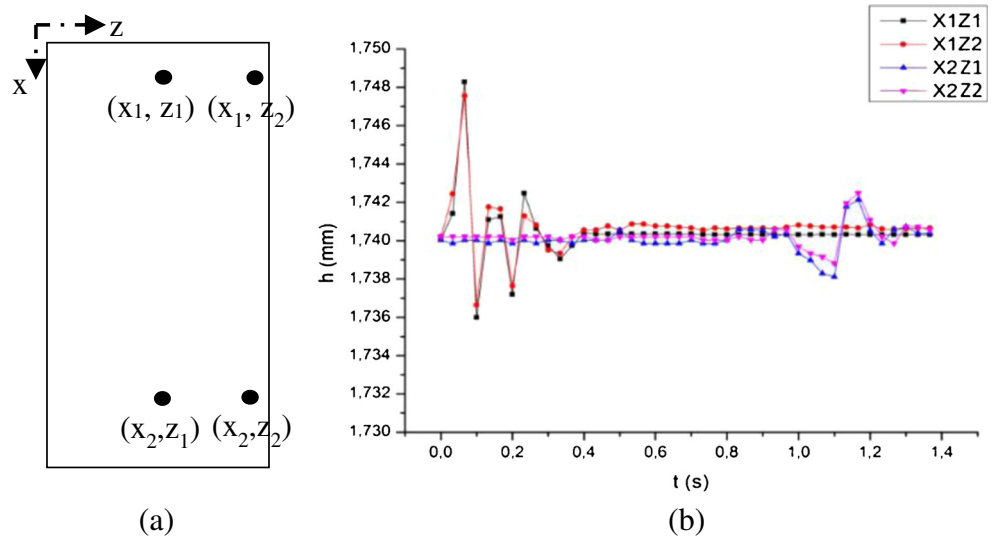
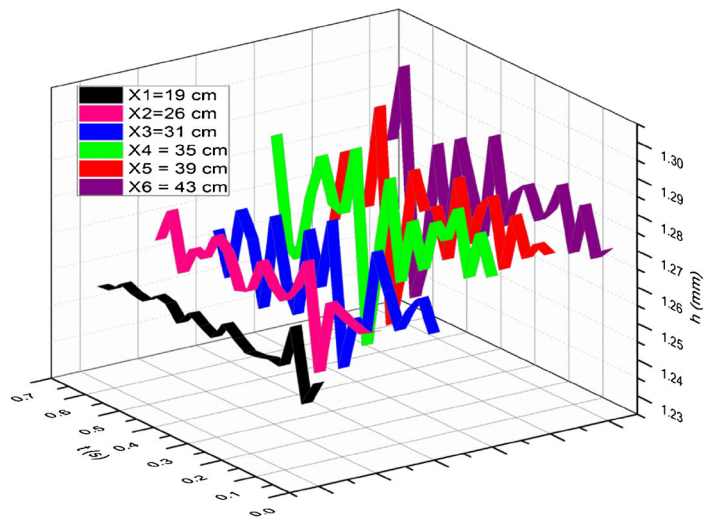
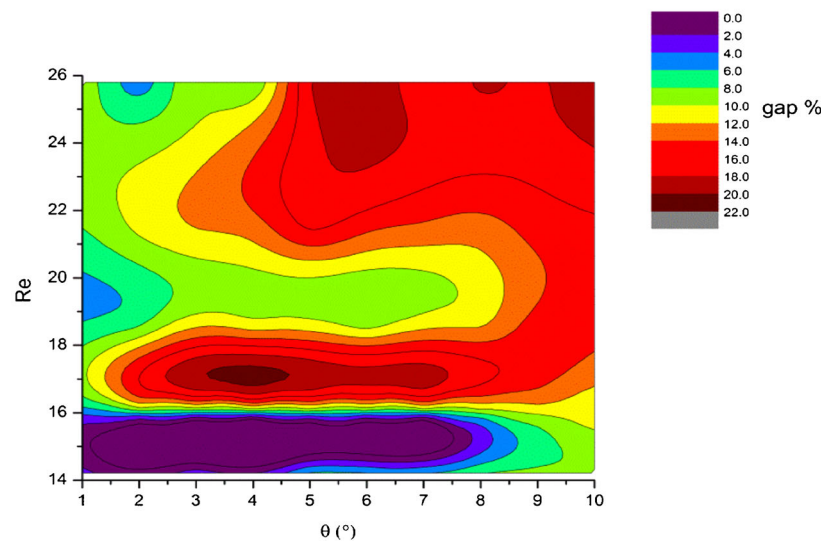


Fig. 8 Liquid film distribution along the inclined plane



(a) Film thickness time evolution for an inclination of 5 degrees at position $X = 19\text{cm}, 26\text{ cm}, 31\text{ cm}, 35\text{ cm}, 39\text{ cm}$ and 43cm for $Re = 25.7$.



(b) Discrepancy, on the film thickness, between theory and experiment.

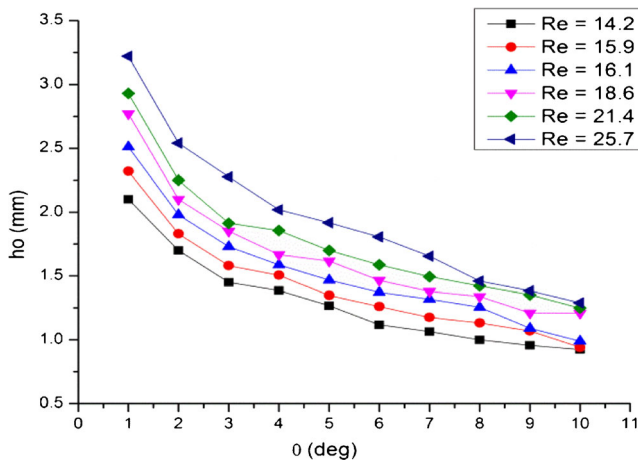
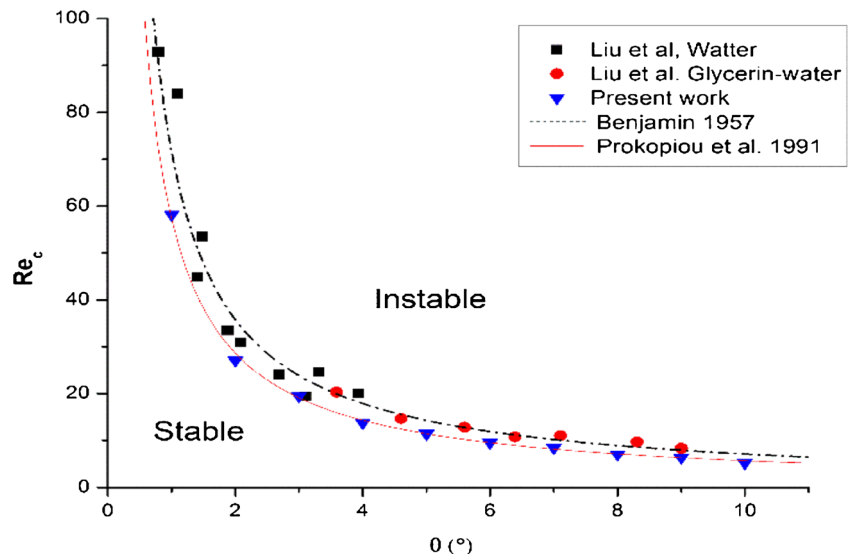


Fig. 9 Liquid film thickness at $x = 26$ cm downstream as function of the inclination angle

are no mechanical or thermal noises related to its use. Furthermore, the technique is very sensitive to the smallest interface movements. To ascertain the hydrodynamic origin of the detected instabilities the experimental loop was placed in an isolated chamber to avoid external mechanical noise. Furthermore, the measurements were conducted during a period of time with no significant temperature variation. For a given inclination angle, the volume flow rate was gradually increased (allowing the flow to stabilize at every variation) up to detection of oscillation which should correspond to the detected threshold value of instability. The recorded volume flow rate was then converted into a critical value of the Reynolds number. For each degree of inclination, the same procedure was repeated up to an angle of 10 degrees. All the recorded values for $0 < \theta < 10$, are reported in Fig. 10. The critical Reynolds numbers, for

Fig. 10 Critical Reynolds number for gravity driven liquid film flow



the present experimental data results, seem to be well captured by a single function of θ that is $\cot(\theta)$; the instability threshold is then expressed as:

$$Re_c = \cot\theta \quad \text{for } 0 < \theta \leq 10 \tag{16}$$

This empirical expression confirms the result of Prokopiou et al. [24]. The difference between our result and the one given by Liu et al. [11] is about 25%.

Concluding Remarks

An experimental approach, based on light reflection, is proposed to measure the thickness of a liquid film flowing over an inclined plane at several positions instantaneously. The technique was first validated for a stable liquid film with flat interface using Spectroscopic Ellipsometry. In case of wavy liquid film, a set up was build-up to validate the reflection technique within the range investigated. The reflection technique showed a good agreement in both cases with a maximum relative error less than 3.5% for flat surface liquid film and a mean deviation less than 5% for a wavy interface. An additional assessment was made, for a flat stable interface, by comparing the measured thickness with theoretical results obtained throughout the Nusselt’s model.

The technique is independent of the properties of the fluid and doesn’t require the injection of particles or tracing powders. It gives access to thickness variations and to the most important parameters dealing with wave’s dynamics traveling on liquid interface with a good accuracy (less than $45 \mu\text{m}$).

As an example some experimental data, on the hydrodynamics of a gravity driven liquid film flow, were reported for an inclination ranging from 1° to 10° and a Reynolds number



of 25.7 using LMRT (Laser Multi-Reflection Technique). The sensitivity of the latter allowed detecting the smallest interface deformation that could appear leading to a correlation for the critical Reynolds number. Furthermore, data was generated (Fig. 8(b)) that would allow a user quantify the confidence level on using the Nusselt's model for unstable flow regime. This technique could deal with the variations of the most important parameters controlling the dynamics of the film flow including film thickness at various positions, wave velocity as well as wavelength.

The present technique can be of interest for generating data for modelling purposes and could be applied in various cases including film thickness distribution and temporal variation, for plane photo-bioreactors.

Acknowledgments The Authors would like to acknowledge the team of “Semiconductors Thin Film” of Materials laboratory for their valuable help with the S.E. technique and samples preparations as well as the Optics Laboratory of the physics Faculty of USTHB.

References

- Kapitza PL, Kapitza SP (1949) Wave flow of thin fluid layers of liquid. *Zh Eksp Teor Fiz* 19:105
- Özgü MR, Chen JC, Eberhardt N (1973) A capacitance method for measurement of film thickness in two-phase flow. *Rev Sci Instrum* 44:1714–1716
- Fukano T (1998) Measurement of time varying thickness of liquid film flowing with high speed gas flow by a constant electric current method. *Nucl Eng Des* 184:363–377
- Seleglim P Jr, Hervieu E (1998) Direct imaging of two-phase flows by electrical impedance measurements. *Meas Sci Technol* 9:1492–1500
- Klausner JF, Zeng LZ, Bernhard DM (1992) Development of a film thickness probe using capacitance for asymmetrical two-phase flow with heat addition. *Rev Sci Instrum* 63:3147–3152
- Hurlburt ET, Newell TA (1996) Optical measurement of liquid film thickness and wave velocity in liquid film flows. *Exp Fluids* 21:357–362
- Shedd TA, Newell TA (1998) Automated optical liquid film thickness measurement method. *Rev Sci Instrum* 69:4205–4213
- Shedd TA, Newell TA (2004) Characteristics of the liquid film and pressure drop in horizontal, Annular, Two-phase Flow Through Round, Square and Triangular Tubes. *J Fluids Eng* 126:807–817
- Zhang JT, Wang BX, Peng XF (2000) Falling liquid film thickness measurement by an optical-electronic method. *Rev Sci Instrum* 71:1883–1886
- Chang H (1994) Wave evolution on a falling film. *Annu Rev Fluid Mech* 26(1):103–136
- Liu J, Paul JP, Gollub JP (1993) Measurement of the primary instabilities of film flows. *J Fluid Mech* 220:69–101
- Benjamin TB (1957) Wave formation in laminar flow down an inclined plane. *J Fluid Mech* 2:554–574
- De Oliveira FS, Yanagihara IJ, Pacifico AL (2006) Film thickness and wave velocity measurement using reflected laser intensity. *J Braz Soc Mech Sci Eng* 28:30–36
- Drallmeier JA, Wegener JL, Armaly BF (2010) Developing laminar gravity-driven thin liquid film flow down an inclined plane. *J Fluids Eng* 132(8):081301
- Tibirică CB, do Nascimento FJ, Ribatski G (2010) Film thickness measurement techniques applied to micro-scale two-phase flow systems. *Exp Thermal Fluid Sci* 34:463–473
- Shkadov VY (1967) Wave flow regimes of a thin layer of viscous fluid subject to gravity. *Fluid Dyn* 2(1):29–34
- Jerri AJ (1977) The Shannon sampling theorem—its various extensions and applications: a tutorial review. *Proc IEEE* 65(11):1565–1596
- Woollam, J. A., Hilfiker, J. N., & Synowicki, R. A. (1999). Ellipsometry, variable angle spectroscopic. *Wiley Encyclopedia of Electrical and Electronics Engineering*, 1–10
- Nusselt W (1916) Die Oberflächenkondensation des Wasserdampfes Teil I, II. *Z. VDI*, 27 (541) (1916), pp. 28, 569–576
- Hanrahan, P., & Krueger, W. (1993). Reflection from layered surfaces due to subsurface scattering. In: *Proceedings of the 20th annual conference on Computer graphics and interactive techniques* (pp. 165–174). ACM
- Lan H, Wegener JL, Armaly BF, Drallmeier JA (2010) Developing laminar gravity-driven thin liquid film flow down an inclined plane. *J Fluids Eng* 132(8):081301
- Pruvost J, Le Borgne F, Artu A, Legrand J (2017) Development of a thin-film solar photobioreactor with high biomass volumetric productivity based on process intensification principles. *Algal Res* 21:120–137
- Gjevik B (1970) Occurrence of finite-amplitude surface waves on falling liquid films. *Phys Fluids* 13(N 8):1918–1925
- Prokopiou T, Cheng M, Chang HC (1991) Long waves on inclined films at high Reynolds number. *J Fluid Mech* 222:665–691